



CrossMark
click for updates

Cite this: *RSC Adv.*, 2016, 6, 59155

Received 8th May 2016
Accepted 14th June 2016

DOI: 10.1039/c6ra11962j

www.rsc.org/advances

Microfluidic structures for large-scale manufacture combining photo-patternable materials

L. Raia,^a N. Rondelli,^a M. Bianchessi^a and M. Carminati^{*b}

A novel application of SiNR, a photo-patternable adhesive material, commonly used for wafer bonding, is proposed as a promising option for fabricating, at industrial scale, fully assembled microfluidic devices at wafer level with resolution down to 15 μm . A self-sealing microchamber for real-time PCR analysis combining laminated SiNR dry films with *in situ* photo-patterned hydrogel passive valves is presented.

Introduction

The most common and consolidated fabrication process for the realization of microfluidic devices relies on the fabrication of the microfluidic channels and structures in PDMS by means of replica molding.¹ Usually the assembly is completed by aligning and bonding the PDMS lid with a flat planar substrate (made of glass or silicon, possibly hosting patterned conductors) by means of covalent bonds activated by plasma treatment. Despite its widespread adoption for rapid prototyping, PDMS presents some limitations such as gas permeability, water uptake, solvent compatibility² and low maximum pressure that the elastomer/substrate assembly can sustain (a few atm).³ Moreover, when micrometric alignment between electrical and microfluidic structures is required, the deformability of the elastomer ultimately limits the achievable accuracy.

Aside from these drawbacks, whose impact strongly depends on the specific application and which, in any case, have not prevented it from becoming a successful laboratory standard, here we consider it from the point of view of the industrialization of a microfluidic platform. In this perspective, the major drawback of this realization approach is its limited compatibility with large-scale, automatable industrial manufacturing processes. Thus, in order to tackle this aspect, we present an alternative, simple and scalable approach for the fabrication of microfluidic devices by means of a novel photo-patternable adhesive called SiNR, routinely employed for wafer-to-wafer bonding in microelectronic foundries.

The device, here illustrated as an example of the straightforward SiNR-based fabrication approach, belongs to broad applicative context of biosensing, in particular for quantitative PCR.⁴ The combination of SiNR structures with *in situ* patterned hydrogel valves demonstrates the feasibility of self-sealing

reservoirs for automatic sample storage during real-time PCR (RT-PCR) analysis. In summary, the development of the technology here presented has been motivated by the following relevant trends, which are guiding the industrialization of laboratory-scale prototypes into reliable engineered devices for mass production: (i) search for manufacturing technologies that are automatable at industry scale, (ii) need for standardization of fluidic interconnections⁵ (for sample inlets and interface between disposable microfluidic cartridges and readout instruments), (iii) focus on sample handling functions, integrated on chip, and (iv) minimization of the number of tasks for the end user, granting widespread adoption by non-trained operators.

Photo-patternable adhesive microfluidics

The use of dry films for patterning microfluidics has been already proposed in the literature,^{6–8} demonstrating some advantages with respect to SU-8.⁶ However, since the materials used so far were mainly borrowed from PCB fabrication processes and not often employed, nor optimized, for silicon, the adherence on large silicon wafers proved to be a critical aspect.⁶ The SiNR family comprises a set of photosensitive adhesive polymers produced by Shin-Etsu Chemicals (Japan). It is a siloxane-based (70%) negative photoresist with modified aromatic bonds for thermal curing (around 180 °C) mostly used for dielectric wafer-to-wafer bonding⁹ and MEMS packaging.¹⁰ It can be spun from liquid solution or is available in dry films with thicknesses spanning from 12 μm to 100 μm . The film is patterned and sandwiched between two rigid slides (Fig. 1). In this work the dry SiNR 3570 has been used featuring a thickness of 50 μm . Interestingly, more layers can be laminated on top of the others. In particular, here, two layers have been overlapped in order to achieve a total thickness of 100 μm . During photo-patterning, in our case with a maskless laser writer (model μPG 101 by Heidelberg), a larger thickness simply requires more energy during the exposure to UV light (at 375 nm wavelength): a dose of 1000 mJ cm^{-2} for 50 μm and 2000 mJ cm^{-2} for 100 μm .

^aSTMicroelectronics, Advanced Systems Technology (AST), Via C. Olivetti 2, 20041 Agrate Brianza (MI), Italy

^bPolitecnico di Milano, Dipartimento di Elettronica, Informazione e Bioingegneria (DEIB), P.za Leonardo da Vinci 32, 20133 Milano, Italy. E-mail: marco1.carminati@polimi.it

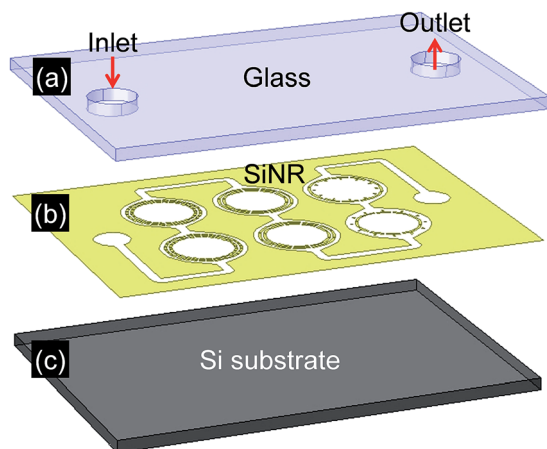


Fig. 1 Microfluidic channels realized in SiNR photo-patternable adhesive sandwiched between two rigid chips (silicon bottom substrate and glass top lid where fluidic connections are drilled prior to bonding).

Usually, the preferred substrate is a silicon wafer. In our case, in order to achieve precise control of the temperature of the fluid inside the chamber during PCR cycles, the silicon substrate (12 mm by 17.7 mm) hosts a large serpentine-shaped resistive heater (115 μm width, 1 k Ω resistance), with a resistive temperature sensor (390 ppm per $^{\circ}\text{C}$) in the middle (Fig. 2) for closed-loop temperature regulation. All these metal lines, made of Al and covered with a 1 μm -thick SiO_2 passivation layer, are defined by standard photolithography on the bottom of an 8" wafer. In this case, the detection of DNA concentration is optical (by means of fluorescence) so the presence of the silicon substrate has no detrimental impact on the limit of detection. Instead, in the case of electrical detection with electrodes fabricated on the bottom layer, the parasitic coupling due to the conductive substrate must be taken into consideration and insulating substrate materials (such as glass and quartz) should be preferred.¹¹

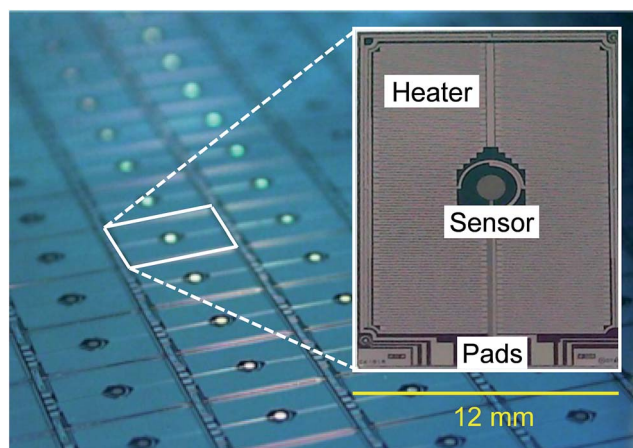


Fig. 2 Active silicon substrate (12 mm by 17.7 mm) of the PCR chambers including resistors for heating and temperature sensing (closed-loop temperature control).

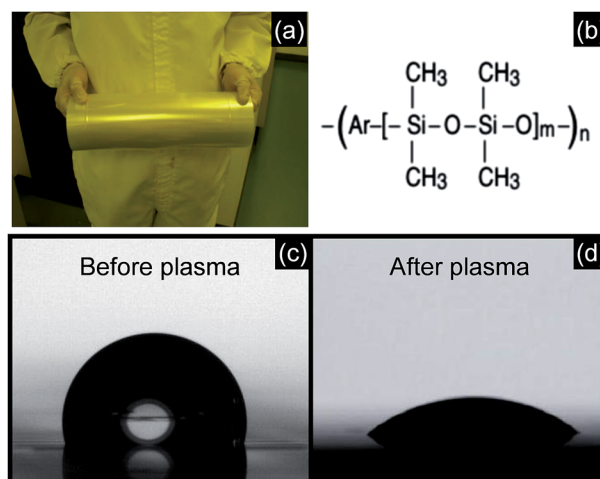


Fig. 3 Features of the SiNR material: (a) foil roll, (b) chemical formula, (c) contact angle of a water droplet as laminated (100°) and (d) after plasma treatment (20°).

The SiNR dry film, available in rolls (Fig. 3a), is applied to the silicon substrate by means of lamination. A standard laminator (model Lamex-325 by GMP with infrared heating up to 150°C and max processable thickness of 3 mm) heated at 80°C is suitable to apply uniformly the SiNR foil to the rigid substrate (with the same uniformity granted by professional laminators, routinely employed in the production lines). The laminator pressure (100 kPa) and speed (680 mm min^{-1}) have been empirically optimized, but are not critical parameters. The top lid is made of borosilicate glass (Pyrex) with a thickness of 500 μm . Inlets and outlets are opened in the glass prior to bonding by means of a diamond drilling tool. Then, a custom-designed hydraulic press is used to perform device bonding. Irreversible bonding of the three layers is achieved at a pressure of 3 bar, a temperature of 150°C and for a duration of 50 min. An additional layer of polycarbonate can be optionally added on

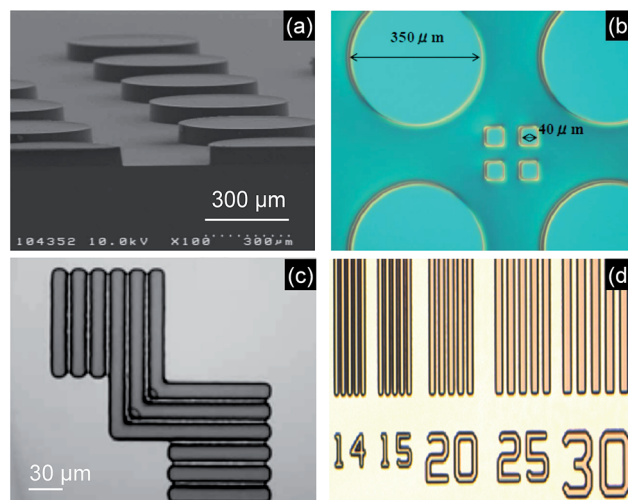


Fig. 4 Examples of patterned micro-structures in SiNR: (a–c) laminated dry film of 50 μm thickness and (d) spin-coated, demonstrating a minimum resolution of about 15 μm (image courtesy of Shin-Etsu).

the top, in order to interface with conical fluidic interconnects (e.g. Luer type) directly built in the plastic. Prior to bonding no special chemical treatment needs to be applied to the silicon substrate to remove the thin native oxide layer, since SiNR bonds equally well both on silicon and silicon dioxide.

After lamination the SiNR layer is hydrophobic (with a contact angle of 100° as visible in Fig. 3c), but thanks to the hydrophilicity of silicon and glass, the channels can be easily filled. Thus, prior to thermo-hydraulic bonding, oxygen plasma (80% O_2 for 40 s at 100 W RF power) is used to remove any residue on the silicon substrate. Immediately after plasma treatment, the contact angle of SiNR is between 20° and 30° (Fig. 3d). After several hours, the effect of plasma treatment vanishes, but the contact angle settles on a lower value (80°) due to a permanent modification of the surface, stable for several weeks.

Although in our application the required patterning resolution is not critical (with the minimum feature being $\sim 50 \mu\text{m}$), this material shows interesting performance. In fact, as illustrated in Fig. 4, for the $50 \mu\text{m}$ dry film, the resolution is between 40 and $15 \mu\text{m}$. Instead, with a thin layer ($3 \mu\text{m}$) of the same material in liquid formulation (SiNR-3750HS6) deposited by spin coating, a resolution of $10 \mu\text{m}$ can be achieved. The steps of the straightforward fabrication flow starting from the SiNR dry film are summarized in Fig. 5.

Finally, SiNR presents excellent mechanical properties. Its Young's modulus is significantly higher than that of PDMS (360–870 kPa), but of course lower than silicon (190 GPa). In fact, it can be tuned from 100 MPa to 1.4 GPa by changing the content of siloxane, respectively from 70% (in SiNR-3170) to 10% (SiNR-3110). The coefficient of thermal expansion is 80–180 ppm per $^\circ\text{C}$ and, after curing, the shrinkage is less than 10%. In particular, for the product that we employed (SiNR-3570 that is an evolution of 3170 modified for bonding at lower temperature), the adhesion strength on a silicon wafer is 11.7 MPa for the dry film and 11.2 MPa for the spin-on formulation. This value is about 20-time larger than the maximum bonding strength reported for the standard PDMS/glass interface.¹²

Self-sealing microchamber for real-time PCR

We now focus on the fabrication of a specific microfluidic device, aimed at real-time PCR analysis,⁴ representing an example of application of this fabrication technology, as well as of the compatibility with *in situ* photo-patterning of hydrogel-based actuators. The device consists of a set of microchambers aligned with the silicon substrate for precise temperature cycling (Fig. 2) and coupled to an imaging system. The RT-PCR measurement protocol includes the following steps: initial chamber filling with the sample and PCR reagents, chamber sealing, initial denaturation (95°C for 2 min) then iteration of 40 cycles of denaturation (95°C for 5 s), annealing (60°C for 30 s) and fluorescent signal acquisition.

Surface wettability is particularly relevant here, since the device should be automatically filled by capillarity when a droplet of the sample is simply pipetted at the inlet. No pumps are used to fill the device, meant as a disposable cartridge for the analysis of nucleic acids. Fig. 6 shows the straightforward self-filling with coloured water of a test fluidic system (100 μm -thick) consisting of the cascade of few circular microchambers, compatible with the volume of samples for PCR application (diameter 1330 μm with 12 equally-spaced inlets of width 50 μm) and connected by single channel. This annular shape has been chosen in order to avoid corners and recesses that are the most critical locations where bubbles might get trapped, seriously compromising the device operation. The fluid speed in the straight channel is about 10 mm s^{-1} , leading to a complete device filling time of $\sim 2 \text{ s}$.

Hydrogel passive valves

Once the PCR microchamber has been designed and experimentally validated, hydrogels are selected as the ideal solution for self-sealing of DNA samples to be amplified, after loading

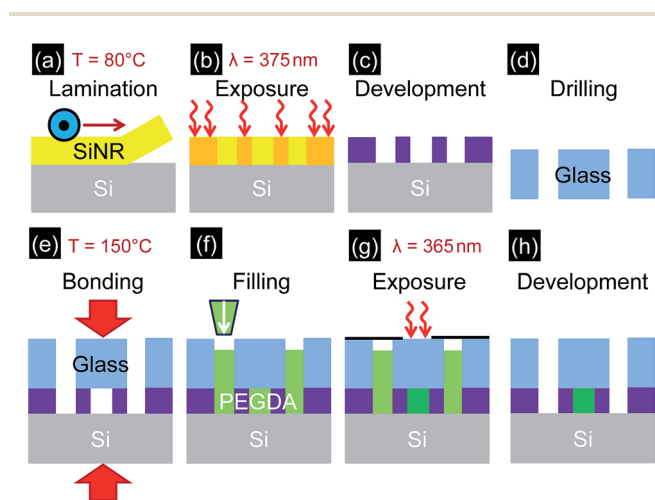


Fig. 5 Process flow of the SiNR device fabrication: (a–e) microfluidic structure patterning, (f–h) *in situ* fabrication of hydrogel (PEGDA) valves.

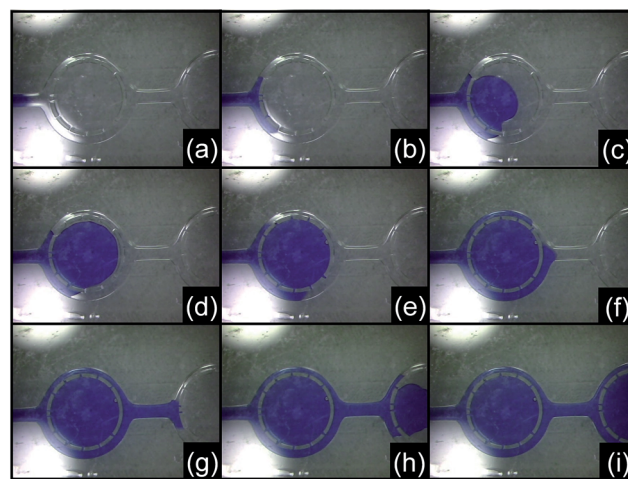


Fig. 6 Passive self-filling sequence (with blue-coloured water) of the microchamber fabricated in SiNR demonstrating good capillarity after plasma treatment.

inside the chambers. Among different hydrogels, PEGDA (Sigma Aldrich, low molecular weight of 575 Da) has been selected thanks to its biocompatibility, non-fouling surface (low adhesion of proteins), large adoption in biomedicine and ease of manipulation. As shown by Beebe and co-workers¹³ it is possible to realize simple valves requiring no external source of power, by local photo-polymerization of PEGDA. Consequently, after bonding, the SiNR microfluidic channels and chambers are filled with the liquid precursor of PEGDA (DMPA). Then, photo-patterning is achieved through the top glass layer that is transparent to UV light (375 nm) used for reticulation (Fig. 3f–h). Hydrogel reticulation inside a non-permeable microfluidics allows: (i) avoiding the presence of oxygen that inhibits the reaction and (ii) obtaining PEGDA structures with the same height of the SiNR structures.

Normally-open valves consist of structures that are separated in dry condition and eventually close due to PEGDA swelling when a liquid sample is injected.^{14,15} In order to improve sealing, after valves closing, mineral oil can be injected to prevent evaporation and grant confinement over long term operation.

Two design parameters have been optimized: the geometrical dimensions and the hydrogel concentration (water/PEGDA dilution ratio). Fig. 7 shows preliminary valve experiments where the PEGDA is sandwiched between two fixed SiNR curved walls of the same length. Different lengths of a slab of PEGDA (width of 100 μm) have been tested, as shown in Fig. 8, showing a relative linear swelling which decreases with a negative slope of $\sim 1\%$ per 100 μm in the 100–500 μm range. The deviation of data in Fig. 8 from the linear fitting is less than 0.5%, which for a slab of 200 μm corresponds to an error of 1 μm that is definitely tolerable, being below the resolution of the lithography.

The valve aperture is 50 μm wide (Fig. 9). The two PEGDA side walls expand closing and sealing this opening. Consequently, each of the two should expand for a minimum stroke of 25 μm . An optimal value of the length of the PEGDA slab, *i.e.* an optimal value of the linear swelling, exists since, for short

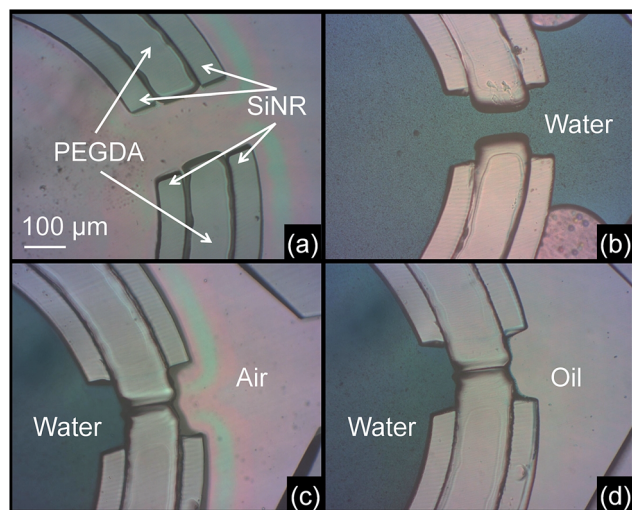


Fig. 7 Self-sealing of a valve based on PEGDA hydrogel between two SiNR guides upon filling with water. After closure, air and oil replace water outside the chamber.

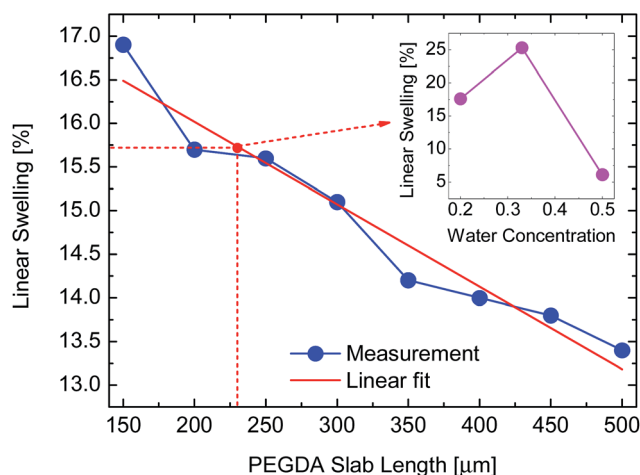


Fig. 8 Experimental investigation of the swelling of PEGDA slabs (100 μm wide) of different lengths and for different water volume concentrations (inset).

lengths, the sealing will not be tight, while for excessively long lengths, the pressure would be too high, producing bending and thus again leakage. We have empirically identified an optimal PEGDA length of 230 μm which corresponds to a total expansion stroke of about 25%, *i.e.* 57 μm (29 μm per side) as illustrated in Fig. 8, thus slightly larger than the minimum of 25 μm . Fig. 8 shows that, in order to achieve a given stroke, two parameters of the PEGDA can be optimized: the slab length and its water concentration (inset). Choosing a length of 230 μm and a water volume concentration of 33% (50 μL of water and 100 μL of PEGDA), we obtain the desired linear swelling of 25%.

The layout of the final device featuring 12 valves and a diameter of 1.3 mm (sample volume of 0.4 μL) is shown in Fig. 9. In order to reduce the friction with the fixed walls, an asymmetric structure has been chosen, consisting of an outer curved wall (separated from the adjacent segments by 50 μm) and of an inner pillar anchoring only the middle of the PEGDA slab. The valve

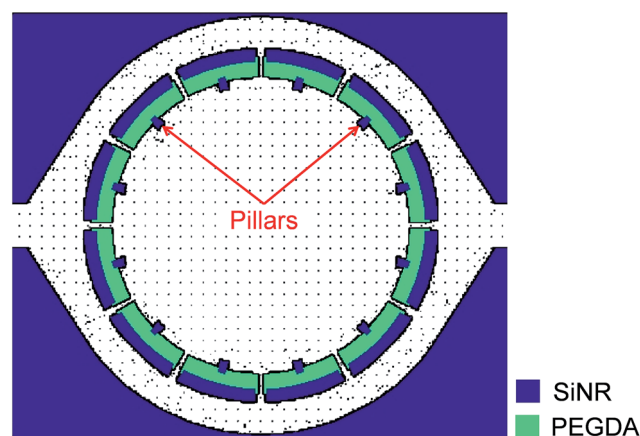


Fig. 9 Layout of the circular PCR microchamber (diameter 1.33 mm, volume 0.44 μL) comprising 12 self-sealing hydrogel passive valves optimized in terms of wall friction.

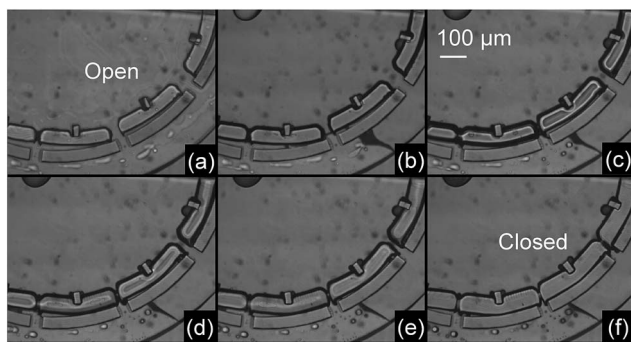


Fig. 10 Self-closing sequence of the valve, each frame is sampled every 10 seconds for a total closing time of 60 s.

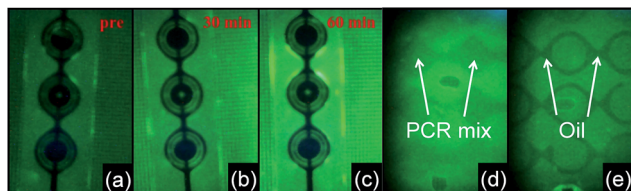


Fig. 11 Assessment of auto-fluorescence levels in different conditions of the fabricated chip: empty (a) before thermal bonding, (b) 30 minutes and (c) 60 minutes after bonding, (d) filled with PCR mix and (e) during PCR thermal cycling sealed with mineral oil.

temporal operation is reported in Fig. 10: complete chamber self-closing is obtained in approximately 1 minute.

Auto-fluorescence assessment

Since in the context of quantitative PCR, detection is commonly performed by means of fluorescence, an important aspect concerns the assessment of the auto-fluorescence level of this material and its compatibility with detection systems (in this case, in particular, with the Q3 real-time PCR platform by STmicroelectronics⁴ tuned to detect green fluorescence of the SYBR Green marker). Despite some fluorescence is apparent at 520 nm wavelength (probably due to the SiNR aromatic rings, similar to the five aromatic rings present in the SYBR molecule), as visible in Fig. 11, it is possible to distinguish the solution in the chambers with respect to the walls. Outside of the emission band of CYBR green, no significant fluorescence was detected.

Conclusions

We have presented an original application of an industrial adhesive for the realization of robust photo-patternable micro-fluidic structures, with a resolution of a few tens of μm . With respect to the consolidated PDMS-based fabrication technique,

this technology offers lower deformability and better compatibility with industrial manufacturing. In fact, all the key steps of this fabrication process (including lamination, patterning and bonding) are suitable for automatization. Bonding can be performed at wafer level and fully assembled devices can be singulated at the very end of the process, thus enabling efficient device handling and scalability to large volumes. Differently from previously prosed dry films, the SiNR grants excellent adhesion on silicon wafers, good mechanical and thermal properties and limited shrinkage. Of course, the relevance of these advantages significantly depends on the final application.

Interestingly, the application of the SiNR dry film on a silicon substrate at relatively low temperature ($80\text{ }^{\circ}\text{C}$ lamination, $150\text{ }^{\circ}\text{C}$ bonding) is also compatible with CMOS active substrates, thus representing a promising solution for CMOS/fluidics coupling, as well as for advanced hybrid packaging. This technology, here demonstrated in a specific proof-of-concept case in combination with passive hydrogel valves for confinement of DNA samples and thermal cycling for quantitative PCR analysis, is suitable for a broad range of applications, including micro-fluidics for cell culturing,¹⁶ drug delivery¹⁷ and drug discovery.¹⁸

References

- 1 S. Neethirajan, I. Kobayashi, M. Nakajima, D. Wu, S. Nandagopal and F. Lin, *Lab Chip*, 2011, **11**, 1574.
- 2 R. Mukhopadhyaya, *Anal. Chem.*, 2007, **79**, 3248.
- 3 E. Sollier, C. Murray, P. Maoddi and D. Di Carlo, *Lab Chip*, 2011, **11**, 3752.
- 4 N. Marziliano, *et al.*, *Clin. Chim. Acta*, 2015, **451**, 240.
- 5 C. M. Klapperich, *Expert Rev. Med. Devices*, 2009, **6**, 211.
- 6 P. Vulto, *et al.*, *Lab Chip*, 2005, **5**, 158.
- 7 Y. C. Tsai, *et al.*, *J. Chromatogr. A*, 2006, **1111**, 267.
- 8 I. Chartier, *et al.*, *Proc. SPIE*, 2003, **4982**, 208.
- 9 W. W. Flack, H. Nguyen and E. Capsuto, *Proc. SPIE*, 2006, 6153.
- 10 V. Dragoi, E. Cakmak, E. Capsuto, C. McEwen and E. Pabo, *Proc. SPIE*, 2009, 7362.
- 11 M. Carminati, M. Vergani, G. Ferrari, L. Caranzi, M. Caironi and M. Sampietro, *Sens. Actuators, B*, 2012, **174**, 168.
- 12 C. W. Beh, W. Zhou and T.-H. Wang, *Lab Chip*, 2012, **12**, 4120.
- 13 D. J. Beebe, *et al.*, *Nature*, 2000, **404**, 588.
- 14 D. Kim, *et al.*, *Lab Chip*, 2007, **7**, 193.
- 15 Y. T. Chen, *et al.*, *RSC Adv.*, 2016, **6**, 44425.
- 16 M. Vergani, *et al.*, *IEEE Transactions on Biomedical Circuits and Systems*, 2012, **6**, 498.
- 17 B. Ziaie, A. Baldi, M. Lei, Y. Gu and R. A. Siegel, *Adv. Drug Delivery Rev.*, 2004, **56**, 145.
- 18 C. Caviglia, *et al.*, *Anal. Chem.*, 2015, **87**, 2204.